ARTICLE

Synthesis and Properties of $Pr_{1-x}Rb_xMnO_3$ ($0.05 \leq x \leq 0.08$) with Perovskite-Type Structure

Dong Wang, Kai-bin Tang*, Zheng-hua Liang, Yan-xiang Nie

Hefei National Laboratory for Physical Sciences at Microscale, Department of Chemistry, University of Science and Technology of China, Hefei 230026, China

(Dated: Received on June 25, 2010; Accepted on October 11, 2010)

Rb-substituted $Pr_{1-x}Rb_xMnO_3$ ($0.05 \leq x \leq 0.08$) was successfully synthesized by solid state reaction. Powder X-ray diffraction showed that all the compounds were orthorhombic with the space group of *Pnma*. Spin glass behaviors were observed for all the compounds at low temperature, suggesting the competition between ferromagnetic and antiferromagnetic. The temperature dependence of the resistivity for the compound $Pr_{0.92}Rb_{0.08}MnO_{3.02}$ at 0 and 2 T magnetic field was also investigated. The compound shows semiconducting behavior, and the band gap is 0.3 eV. The maximum magnetoresistance is about 30% at 2 T magnetic field near 116 K.

Key words: Perovskite, Spin glass behavior, Semiconductor, Magnetoresistance

I. INTRODUCTION

In the last several decades, there has been a great interest in the development of new materials with the Mn containing perovskite structure because of their uniquely magnetic and electrical properties. Stoichiometric $LaMnO_3$ shows antiferromagnetic and semiconducting behavior, while $La_{1-x}A_xMnO_3$(A=Ca, Sr, Ba and Pb) shows a paramagnetic to ferromagnetic transition coupled with an insulator to metal transition. This transition was first reported by Jonker and Vansanten [1, 2] and was also found for their rare-earth homologues. Zener proposed the mechanism of this transition on double exchange interaction [3]. The origin of the ferromagnetism is due to the order of spin moment S=3/2 in the $3d_\varepsilon$ obital of Mn via transfer of the $3d_\gamma$ electrons through the $2p_\sigma$ orbital of the oxygen ion located at the center of two Mn ions in the perovskite type structure.

Another remarkable property of these compounds is the so-called colossal magnetoresistance (CMR) [4−13]. CMR is a property of some materials, mostly manganese-based perovskite oxides, that enables them to dramatically change their electrical resistance in the presence of a magnetic field. The magnetoresistance of conventional materials enables changes in resistance of up to 5%, but materials featuring CMR may demonstrate resistance changes by orders of magnitude. For example, in bulk $La_{1-x}Sr_xMnO_3$, a reduction of resistance with more than three orders in magnitude is reported [4].

Recently alkali mental substituted $LnMnO_3$ have also been studied. Because of its +1 valence state, alkali metal can induce the increase in valence state of Mn more efficiently. $La_{1-x}A_xMnO_3$ (A=Na, K, or Rb) systems reported by Shimura *et al.* [14] showed similar properties to divalent ion substituted lanthanum manganites. Na- and K-substituted $PrMnO_3$ have also been studied by Jirak *et al.* and Shivakumara *et al.* [15, 16]. In this work, Rb-doped $PrMnO_3$ was prepared, and its electrical and magnetic properties were investigated.

II. EXPERIMENTS

$Pr_{1-x}Rb_xMnO_3$ compounds were prepared by a conventional solid state reaction method. Pr_6O_{11} (99.9%, Sinopharm Chemical Reagent Co., Ltd.), Rb_2CO_3 (99.5%, Sichuan State Lithium Materials Co., Ltd.) and $MnCO_3$ (99%, Sinopharm Chemical Reagent Co., Ltd.) were weighted in the nominal compositions of $Pr_{1-x}Rb_xMnO_3$ (x=0.05, 0.10, 0.15) with an excess of 100% of Rb_2CO_3 to compensate the loss due to evaporation. The mixed powders were calcined in air at 850, 1000, and 1100 °C for 24 h with intermediate grinding, and then were pressed into pellets and sintered at 800 °C for 48 h in the oxygen flow. Finally, the products were washed with hot distilled water to eliminate soluble impurities and dried at 120 °C in air.

Phase analysis of the products was examined by X-ray diffraction (XRD) using a Philips X'pert Pro Super X-ray diffractometer with Cu Kα radiation (λ=1.54187 Å) at room temperature (40 kV, 30 mA). The XRD data for indexing and cell-parameter calculation were collected in a continuous scan mode with a

*Author to whom correspondence should be addressed. E-mail: kbtang@ustc.edu.cn, FAX: +86-551-3606266

TABLE I Composition, lattice parameters (a, b, c and V) and content of Mn^{4+} of $Pr_{1-x}Rb_xMnO_3$.

Initial Pr content	Final composition	a/Å	b/Å	c/Å	V/Å^3	Content of Mn^{4+}
0.95	$Pr_{0.95}Rb_{0.05}MnO_{2.98}$	5.5299	7.7218	5.4783	233.928	5.2%
0.90	$Pr_{0.94}Rb_{0.06}MnO_{3.02}$	5.4862	7.7298	5.4841	232.565	15.0%
0.85	$Pr_{0.92}Rb_{0.08}MnO_{3.02}$	5.4839	7.7235	5.4720	231.766	20.4%

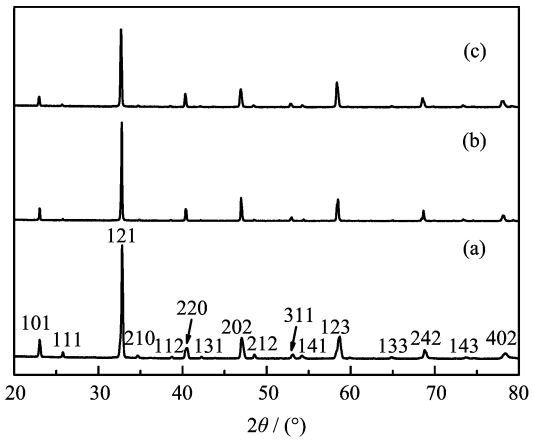

FIG. 1 Powder XRD patterns of (a) $Pr_{0.92}Rb_{0.08}MnO_{3.02}$, (b) $Pr_{0.94}Rb_{0.06}MnO_{3.02}$, (c) $Pr_{0.95}Rb_{0.05}MnO_{2.98}$.

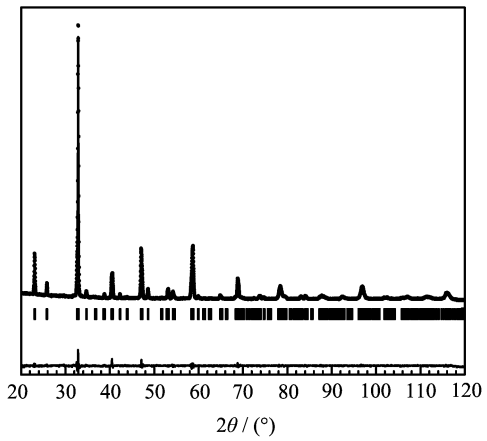

FIG. 2 Observed (dots), calculated (solid line) and difference (bottom) XRD patterns for $Pr_{0.92}Rb_{0.08}MnO_{3.02}$.

step size of 0.017° in the angular range $20°<2\theta<120°$. The XRD patterns were analyzed by the Rietveld method using the FULLPROF program [17].

The compositions of the compounds were determined by energy dispersive X-ray (EDX) spectroscopy on a JEOL-2010 transmission electron microscope at an acceleration voltage of 200 kV. The actual Mn^{4+} and oxygen content was determined by the redox titration based on the reduction of Mn^{3+} and Mn^{4+} by Fe^{2+} with the method of Bloom *et al.* [18]. The magnetic measurements were measured in commercial physical property measurement system (PPMS, quantum design). The temperature dependence of the resistivity for the compound $Pr_{0.92}Rb_{0.08}MnO_{3.02}$ was measured by a standard four-probe method.

III. RESULTS AND DISCUSSION

A. XRD analysis

The X-ray diffraction patterns of all the compounds reveal that no impurities exist with the initial Pr content from 0.95 to 0.85 ($0.05\leq x\leq 0.15$). When $x>0.15$, Mn_3O_4 impurity was observed in the XRD pattern. However, EDX analysis showed that the Rb content of substitution was less than our expectation, and the maximum Rb substitution was 0.08 with the initial Pr to Mn ratio 0.85:1.0 (Table I). The excess Mn seems to be converted into a soluble manganese salt with the excess Rb, since it was found that the distilled water used for washing the products became red-brown quickly in air, moreover, we do not see any detectable impurity phases containing manganese in the XRD patterns. Thus, the range over which single phase compounds could be produced proved to be extremely narrow ($0.05\leq x\leq 0.08$) (Table I). This substitution difficulty was also found in other alkali ion substituted lanthanum manganites [15, 16]. It is probably due to the discrepancy of the Pr^{3+} and Rb^+, especially the large difference in the ionic radii between Pr^{3+} ($r_{Pr^{3+}}$=1.18 Å, CN=9) and Rb^+ (r_{Rb^+}=1.63 Å, CN=9) [19].

The lattice parameters of the compounds are summarized in Table I and their XRD patterns are shown in Fig.1. All the compounds can be indexed in the orthorhombic structure with the space group Pnma. The space group of the compounds was confirmed using the FULLPROF program. The observed, calculated and difference of the XRD patterns, for $Pr_{0.90}Rb_{0.10}MnO_3$ are given in Fig.2, and the observed pattern is in agreement with the calculated one. The conventional reliability factors, profile factor R_p, weighted profile factor R_{wp}, expected weighted profile factor R_{exp}, Bragg factor R_B, and crystallographic factor R_F for the compounds are 12.32%, 11.74%, 6.76%, 3.20%, 3.48% (x=0.05); 12.83%, 12.46%, 6.47%, 4.2%, 4.56% (x=0.06), and 11.56%, 10.84%, 5.04%, 4.19%, 4.08% (x=0.08), respectively. From Table I it can be seen that the unit cell volume decreases with increasing

DOI:10.1088/1674-0068/23/06/726-730

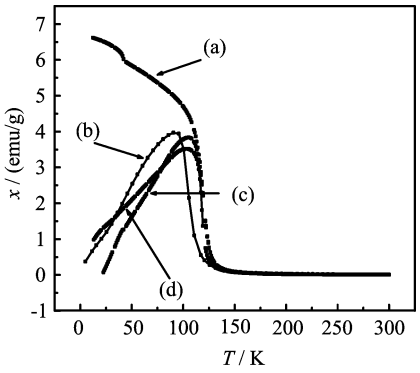

FIG. 3 Magnetic susceptibility plots as a function of temperature of $Pr_{1-x}Rb_xMnO_3$. (a) $Pr_{0.92}Rb_{0.08}MnO_3$(FC), (b) $Pr_{0.95}Rb_{0.05}MnO_3$(ZFC), (c) $Pr_{0.92}Rb_{0.08}MnO_3$(ZFC), (d) $Pr_{0.94}Rb_{0.06}MnO_3$(ZFC).

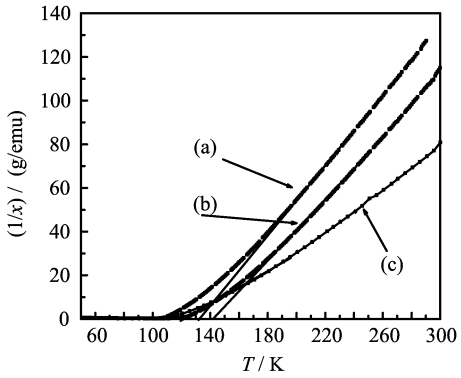

FIG. 4 inverse susceptibility plots as a function of temperature of $Pr_{1-x}Rb_xMnO_3$. (a) $Pr_{0.94}Rb_{0.06}MnO_3$, (b) $Pr_{0.92}Rb_{0.08}MnO_3$, and (c) $Pr_{0.95}Rb_{0.05}MnO_3$.

Rb ion doping. This phenomenon was also observed in other alkali mental substituted $LnMnO_3$ [15, 16]. The ionic radii of Mn^{4+} ($r_{Mn^{4+}}$=0.53 Å, CN=6) is smaller than Mn^{3+} ($r_{Mn^{3+}}$=0.58 Å, CN=6) [19]. In the $Pr_{1-x}Rb_xMnO_3$, the content of Mn^{4+} increases with increasing Rb content, which result in the volume decrease of the $Pr_{1-x}Rb_xMnO_3$.

B. Magnetic properties

Figure 3 shows the magnetic susceptibilities as a function of temperature for $Pr_{1-x}Rb_xMnO_3$ at 100 Oe magnetic field. From Fig.3 we can find that the zero-field cooled (ZFC) and field cooled (FC) curves split up at about 130 K. Below 130 K with the decrease of the temperature the magnetic susceptibilities of ZFC curves increase gradually and reach the maximums then decrease. The divergence of the ZFC and FC curves together with the maximums of the ZFC curves suggests that at lower temperatures the compounds show spin glass behavior. At higher temperatures, the compounds are paramagnetic. The temperature at maximum of ZFC curvers is called spin-freezing temperature (T_f). The T_f of the compounds are 90 K (x=0.05), 103 K (x=0.06), and 106 K (x=0.08) respectively. Spin glass behavior is associated with frustrated systems, resulting from competing interactions. There are Mn^{3+} and Mn^{4+} in $Pr_{1-x}Rb_xMnO_3$. Superexchange interactions between Mn^{3+}/Mn^{3+} and between Mn^{4+}/Mn^{4+} would be antiferromagnetic, whereas superexchange or double exchange involving Mn^{3+}/Mn^{4+} would be ferromagnetic. These interactions between disordered Mn^{3+} and Mn^{4+} could give rise to frustration and spin glass behavior.

Plots of inverse susceptibility *vs.* temperature for $Pr_{1-x}Rb_xMnO_3$ are shown in Fig.4. Plots are linear above 180 K, indicating that the compounds are paramagnetic in this temperature range. The Curie-Weiss

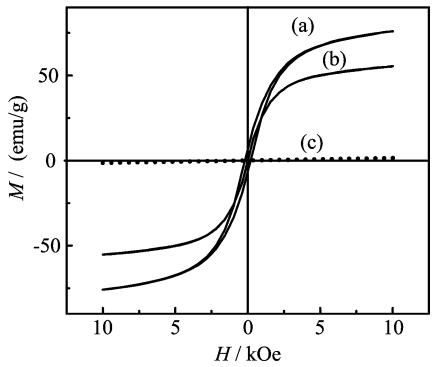

FIG. 5 *M-H* loops at different temperatures for $Pr_{0.92}Rb_{0.08}MnO_{3.02}$. (a) 5 K, (b) 80 K, and (c) 250 K.

constant (θ_p) of the compounds are 121 K (x=0.05), 133 K (x=0.06), and 142 K (x=0.08), respectively. The positive values of the θ_p suggest that ferromagnetic exchange is dominant in the low temperature range. Figure 5 shows *M-H* loops for $Pr_{0.92}Rb_{0.08}MnO_{3.02}$ at different temperatures. The hysteresis loop measured at 5 K displays a typical ferromagnetic behavior and the coercivity force is determined to be 193 Oe (Fig.5(a)). While at 80 K, the coercivity force for the compound is determined to be 11 Oe, which is much smaller than that at 5 K (Fig.5(b)). At higher temperature of 250 K, the linear behavior is observed, because the system has already been in paramagnetic state (Fig.5(c)). Thus, for these compounds, the low temperature state can be described as a ferromagnetic spin glass [20].

C. Electrical properties

The electrical resistivity measured *vs.* temperature with the four probe method shows that all the compounds were semiconducting. Figure 6 shows the temperature dependence of the resistivity for the

DOI:10.1088/1674-0068/23/06/726-730

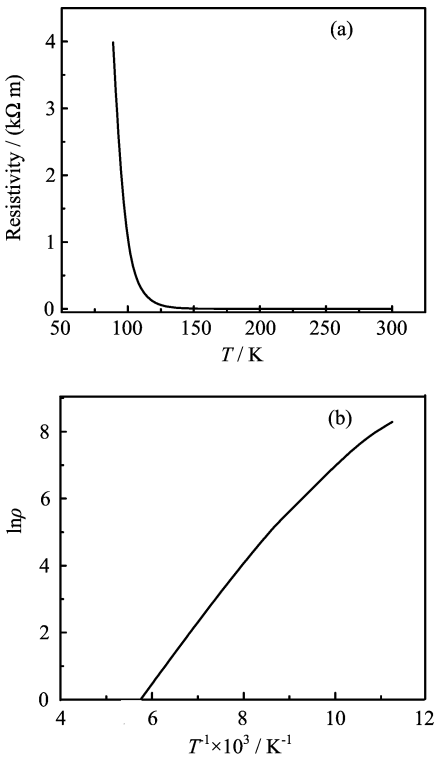

FIG. 6 (a) Temperature dependence of the resistivity for $Pr_{0.92}Rb_{0.08}MnO_{3.02}$. (b) ln$\rho$ dependence of T^{-1} for $Pr_{0.92}Rb_{0.08}MnO_{3.02}$.

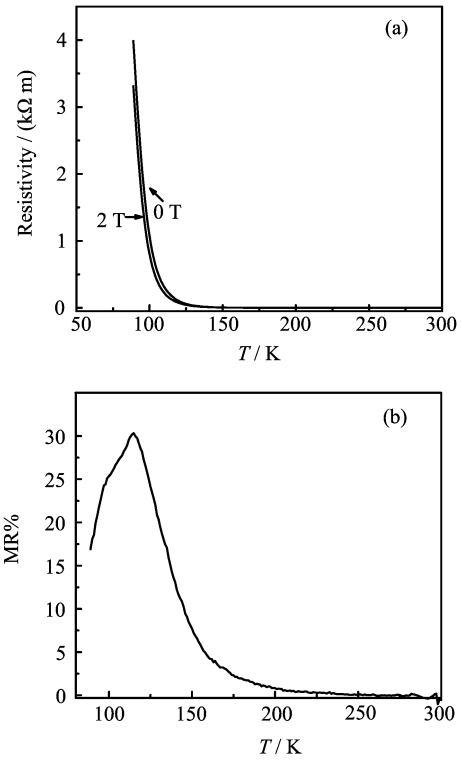

FIG. 7 (a) Temperature dependence of the resistivity for $Pr_{0.92}Rb_{0.08}MnO_{3.02}$ at 0 and 2 T magnetic fields. (b) The plot of MR% *vs.* T of $Pr_{0.92}Rb_{0.08}MnO_{3.02}$.

$Pr_{0.92}Rb_{0.08}MnO_{3.02}$. At low temperature, the compound is insulating. The insulator-mental transition was not found. This may be related to the substitution difficulty which comes from the discrepancy of the Pr^{3+} and Rb^+ valencies and the large difference in the ionic radii between Pr^{3+} and Rb^+. Further more, Shivakamara *et al.* found that, at low temperature, the compounds crystallized in orthorhombic structures are insulators and those crystallized in rhombohedra structure will show an insulator-metal transition [16]. This phenomenon was also observed in our compounds. They are all orthorhombic structures and insulators at low temperature. In Fig.6(b), the lnρ *vs.* T^{-1} plot of $Pr_{0.92}Rb_{0.08}MnO_{3.02}$ is given. The band gap calculated from the slope of Fig.6(b) is about 0.30 eV. Figure 7 shows the temperature dependence of the resistivity for the $Pr_{0.92}Rb_{0.08}MnO_{3.02}$ at 0 and 2 T magnetic fields. Figure 7(a) is the plot of MR% *vs.* T. The MR% is defined as:

$$\mathrm{MR\%} = \frac{R_0 - R_\mathrm{H}}{R_0} \times 100\% \qquad (1)$$

where R_0 and R_H are the resistance at magnetic fields of 0 and 2 T, respectively. From Fig.7(b), we can find the $Pr_{0.92}Rb_{0.08}MnO_{3.02}$ shows a maximum negtive MR% of about 30% near 116 K.

IV. CONCLUSION

$Pr_{1-x}Rb_xMnO_3$ ($0.05 \leq x \leq 0.08$) has been synthesized. Magnetic and electrical properties of these compounds were investigated. The discrepancy of the Pr^{3+} and Rb^+, especially the large difference in the ionic radii between Pr^{3+} and Rb^+ leads to substitution difficulty of these compounds. All the compounds show spin glass behavior at the low temperature. The compounds are all semiconductors. The band gap of $Pr_{0.92}Rb_{0.08}MnO_{3.02}$ is 0.3 eV. The maximum MR% of $Pr_{0.92}Rb_{0.08}MnO_{3.02}$ is about 30% at 2 T magnetic field near 116 K.

V. ACKNOWLEDGMENTS

This work is supported by the National Natural Science Foundation of China (No.20671086) and the National Key Basic Research Special Foundation of China (No.2011CB935900).

[1] G. H. Jonker and J. H. Vansanten, Physica **16**, 337 (1950).
[2] G. H. Jonker, Physica **22**, 707 (1956).

DOI:10.1088/1674-0068/23/06/726-730

[3] C. Zenner, Phys. Rev. **83**, 299 (1951).
[4] R. Von. Helmolt, J. Wecker, B. Holzapfel, L. Schultz, and K. Samwer, Phys. Rev. Lett. **71**, 2332 (1993).
[5] S. Jin, T. H. Tiefel, M. McCorMack, R. A. Fastnacht, R. Ramesh, and H. Chen, Science **264**, 413 (1994).
[6] K. Chahara, T. Ohno, M. Kasai, and Y. Kozono, Appl. Phys. Lett. **63**, 1990 (1993).
[7] M. McCormack, S. Jin, T. H. Fleming, J. M. Phillips, and R. Ramesh, Appl. Phys. Lett. **64**, 3045 (1994).
[8] H. L. Ju, C. Kwon, Q. Li, R. L. Greene, and T. Venkatesam, Appl. Phys. Lett. **65**, 2108 (1994).
[9] S. S. Manoharan, D. Kuman, M. S. Hegde, K. M. Sathyalakshmi, V. Prasad, and S. V. Subramanyam, J. Appl. Phys. **76**, 3923 (1994)
[10] R. Mahendiran, R. Manhesh, A. K. Raychandhuri, and C. N. R. Rao, J. Phys. D **28**, 1743 (1995).
[11] R. Mahendiran, R. Manhesh, A. K. Raychandhuri, and C. N. R. Rao, Phys. Rev. B **53**, 12160 (1996).
[12] B. Raveau, A. Maignan, and V. Caignaert, J. Solid State Chem. **117**, 424 (1995).
[13] V. Caignaert, A. Maignan, and B. Raveau, Solid State Commun. **95**, 357 (1995).
[14] T. Shimura, T. Hayashi, Y. Inaguma, and M. Itoh, J. Solid State Chem. **124**, 250 (1996)
[15] Z. Jirak, J. Hejtmanek, K. Knizek, and R. Sonntag, J. Solid State Chem. **132**, 98 (1997).
[16] C. Shivakumara, M. S. Hegde, T. Srinivasa, N. Y. Vasanthacharya, G. N. Subbanna, and N. P. Lalla, J. Mater. Chem. **11**, 2572 (2001).
[17] J. Rodriguez-Carvajal, *FULLPROF Program: Rietveld Pattern Matching Analysis of Powder Patterns*, ILL Grenoble, (1990).
[18] E. Bloom, T. Y. Kometani Jr., and J. W. Mitchell, J. Inorg. Nucl. Chem. **40**, 403 (1978).
[19] R. D. Shannon, Acta Crystallogr. Sect. A **32**, 751 (1976).
[20] K.V. Rao, M. Fahnle, E. Figueroa, O. Beckman, and L. Hedman, Phys. Rev. B **27**, 3104 (1983).

DOI:10.1088/1674-0068/23/06/726-730